



Discovery of novel purine derivatives with potent and selective inhibitory activity against c-Src tyrosine kinase

He Huang^{a,†}, Jingui Ma^{b,†}, Jianmei Shi^a, Linghua Meng^{b,*}, Hualiang Jiang^a, Jian Ding^b, Hong Liu^{a,*}

^a Drug Discovery and Design Center, State Key Laboratory of Drug Research, Shanghai Institute of Materia Medica, Chinese Academy of Sciences, 555 Zu Chong Zhi Road, Zhangjiang Hi-Tech Park, Shanghai 201203, PR China

^b Division of Anti-tumor Pharmacology, State Key Laboratory of Drug Research, Shanghai Institute of Materia Medica, Chinese Academy of Sciences, 555 Zu Chong Zhi Road, Zhangjiang Hi-Tech Park, Shanghai 201203, PR China

ARTICLE INFO

Article history:

Received 30 March 2010

Revised 11 May 2010

Accepted 12 May 2010

Available online 19 May 2010

Keywords:

c-Src tyrosine kinase

Inhibitor

Purine derivative

Focused library

ABSTRACT

We report here the discovery of novel purine derivatives with potent and selective inhibitory activity against c-Src tyrosine kinase by adopting a strategy integrating focused combinatorial library design, virtual screening, chemical synthesis, and bioassay. Thirty two compounds were selected and synthesized. All compounds showed potent inhibitory activity against c-Src kinase with IC₅₀ values ranging from 3.14 μM to 0.02 μM. Compound **5i** was identified as one of the most potent agent with an IC₅₀ 120 times lower than those of the hits. The high hit rate (100%) and the potency of the new Src kinase inhibitors demonstrated the efficiency of the strategy for the focused library design and virtual screening. The novel active chemical entities reported here should be good leads for further development of purine-based anti-cancer drugs targeting Src tyrosine kinase.

© 2010 Elsevier Ltd. All rights reserved.

1. Introduction

c-Src kinase, a non-receptor tyrosine kinase, is the best understood member of a family of related kinases known as the SFKs (Src family kinases).¹ c-Src play a major role in multiple intracellular signal transduction pathways involved in cell growth, differentiation, survival, adhesion, and migration.^{2–5} It has been demonstrated that Src is overexpressed or constitutively active in a variety of human tumors, including those derived from colon, breast, pancreas, liver, brain, and bladder.^{3,6–9} Moreover, aberrant Src kinase activity is associated with the invasive phenotype in both early and advanced solid tumors.¹⁰ Thus, the discovery of Src kinase inhibitor holds high potential to treat metastatic tumors.^{11–18}

Purine analogs represent an excellent scaffold for targeting many biosynthetic, regulatory, and signal transduction proteins including cellular kinases, G proteins, and polymerases.^{19–31} Figure 1 presents some representative purine derivatives that are potent inhibitors of the c-Src kinase.²¹ Based on the above findings and the availability of abundant substituted purine compounds in our in-house collection, we were intrigued to screening our compounds on Src kinase. One of the exciting screening results is that compounds *N*-(4-methoxyphenyl)-2-(piperazin-1-yl)-9*H*-purin-6-amine (**1a**, Table 1) and *N*-(3-methylphenyl)-2-(piperazin-1-yl)-

9*H*-purin-6-amine (**1b**, Table 1) exhibited moderate inhibitory activity, with the IC₅₀ values of 2.43 μM and 2.42 μM, respectively. Interestingly, they are different from the most reported purine-based Src kinase inhibitors which are often the 2,6,9-trisubstituted purines. Moreover, all the 2,6,9-trisubstituted purines and 6,9-disubstituted purines screened by us showed poor activity against the Src kinase (Table 1).

The focused library and virtual screening have emerged as realizable and cost-effective tools in drug discovery.³² A focused library is built on the basis of a lead molecule or pharmacophore and geared toward one particular molecular target. Generally, extracting fragments from known drugs or ligands (inhibitors or activators) of the studied target is an effective approach for collecting new building blocks.^{7,12,33–35} Meanwhile, druglikeness could be introduced into the library design to reduce its size and increase its efficiency. Herein, we described the discovery of novel purine derivatives with potent and selective inhibitory activity against c-Src tyrosine kinase by adopting a strategy integrated with focused combinatorial library design, virtual screening, chemical synthesis, and bioassay.

2. Materials and methods

2.1. Focused combinatorial library design

The PIPELINE PILOT 7.0 program³⁶ was used in the focused library designing. Having been kept the common moiety of compounds **1a**

* Corresponding authors. Fax: +86 21 50807088 (H.L.), +86 21 50806722 (L.M.).
E-mail addresses: lhmeng@mail.shcnc.ac.cn (L. Meng), hliu@mail.shcnc.ac.cn (H. Liu).

† Two authors contribute equally to this work.

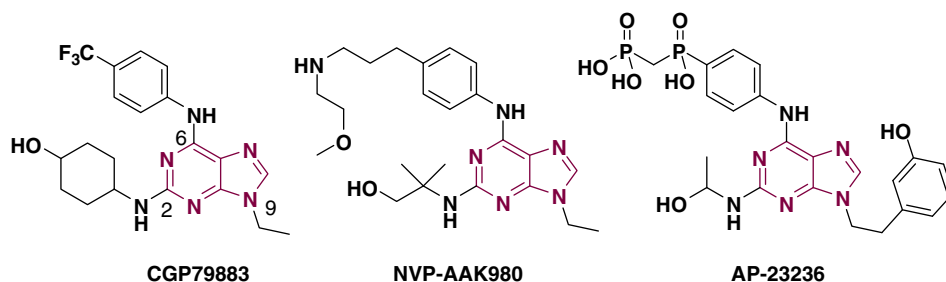


Figure 1. Representative purine-based inhibitors of the Src kinase.

and **1b** of the purine framework, the 2,6-disubstituted purine-based Src kinase inhibitors can be divided into two parts: (A) 6-amines or -anilines substituents; (B) 2-alkyl side chains (Fig. 2). From fragments of Src kinase inhibitors discovered above and previously, 15 fragments for part A, 8 fragments for part B, and 4 frameworks were selected (Fig. 3). These fragments from different parts could react with each other to generate a library containing 480 ($15 \times 8 \times 4$) mole-

cules. The druglikeness of the molecules from the combinatorial library was then evaluated by the druglikeness filter module of PIPELINE PILOT 7.0. The druglikeness descriptor set is composed of the 'Rule of Five' (Num_Atom > 0; N_Count + O_Count \leq 11; Molecular_Weight \leq 500; Num_H_Donors \leq 5; Alog P \leq 2.5). Other parameters used in the PIPELINE PILOT 7.0 were default values. In this way, 308 compounds were filtered for further evaluation.

Table 1

Inhibitory effect of the selected compounds in in-house collection against Src kinase activity by using ELISA assay^a



Compound	R ¹ H	R ²	R ³	IC ₅₀ (μM)	% Inhibition at 10 μM ^b
1a			-H	2.43 ± 0.39	90.5
1b			-H	2.42 ± 0.66	86.6
1c				>10	22.5
1d				>10	16.0
1e				>10	35.8
1f				>10	20.2
1g				>10	10.1
1h				>10	16.4
1i		-H		>10	13.9
1j		-H		>10	6.9
1k		-H		>10	0
PP2^c					99

^a The inhibition rate (%) was calculated using the equation: $[1 - (A_{490}/A_{490 \text{ control}})] \times 100\%$. IC₅₀ values were obtained by Logit method based on the data obtained from three separate experiments; each compound concentration was tested in duplicate. % Inhibition rate at 10 μM.

^b Values are means of three determinations and deviation from the means is <10% of the mean value.

^c PP2 was used as positive control.

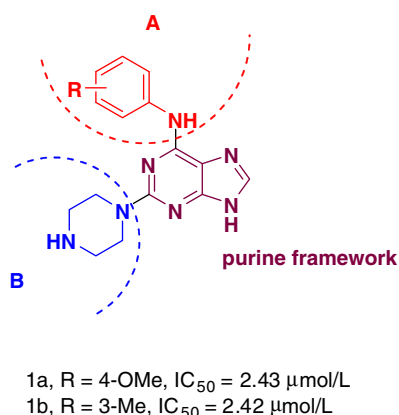


Figure 2. Structures of compounds 1a–b, and three regions of them.

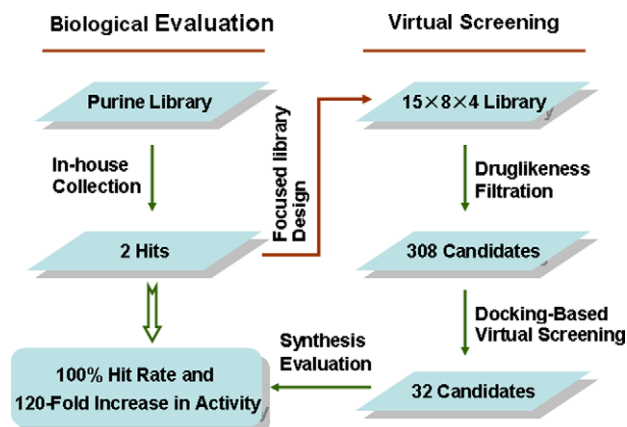


Figure 4. Discovery strategy and experimental flowchart in this study.

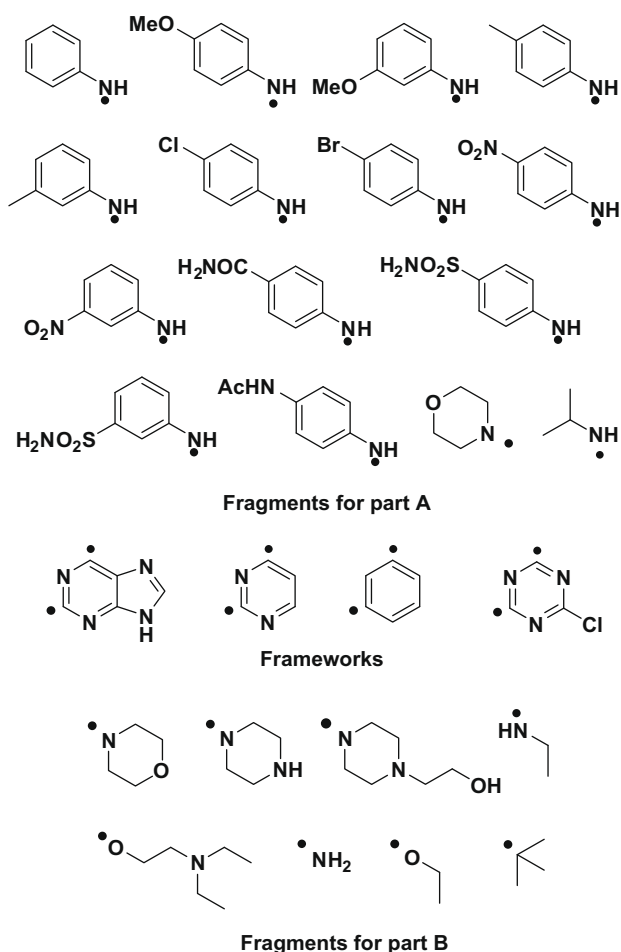


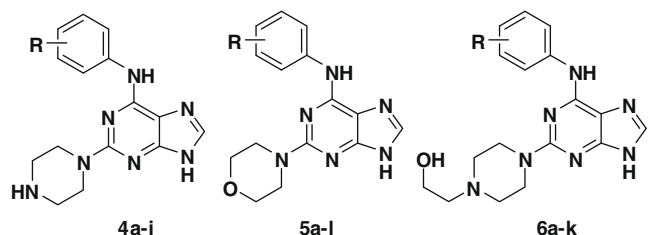
Figure 3. Building blocks for focused library generation. The symbols \cdot represents the sites where fragments connect each other to form a complete structure.

2.2. Virtual screening

A computational docking was performed by using DISCOVERY STUDIO 2.1 (DS 2.1) program³⁷ in order to identify the fragments and the possible interaction between the ligand and the Src kinase. The X-ray crystal structure of Src kinase (PDB entry No.: 1y57) was used as a target for the virtual screening. The binding potential between Src kinase and molecules in the combinatorial library was

Table 2

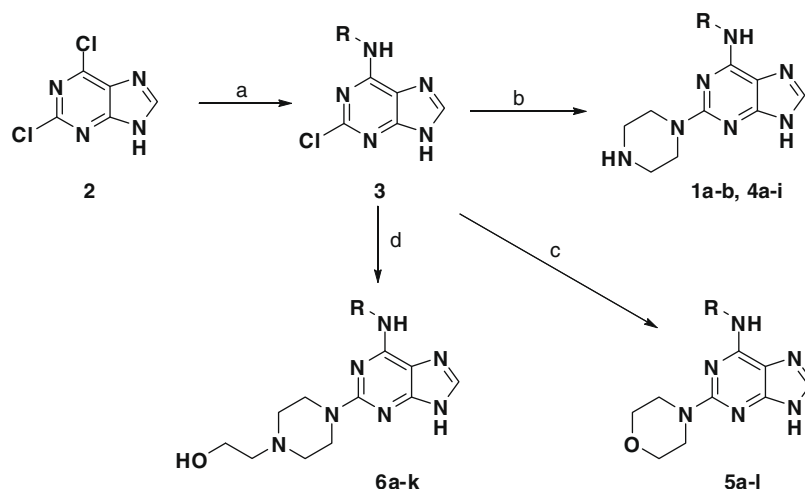
Chemical structures and Src kinase inhibitory activities of compounds 4a–i, 5a–l and 6a–r^a



Compound	R	IC_{50} (μM)
4a	3-Methoxy	1.21 \pm 0.16
4b	4-Chloro	1.18 \pm 0.04
4c	4-Bromo	1.76 \pm 0.33
4d	4-Nitro	1.40 \pm 0.24
4e	3-Nitro	0.95 \pm 0.53
4f	4-Aminosulfonyl	1.82 \pm 0.02
4g	3-Aminosulfonyl	0.10 \pm 0.04
4h	4-Carbamoyl	2.20 \pm 0.07
4i	4-Acetamido	1.05 \pm 0.47
5a	H	0.75 \pm 0.20
5b	4-Methoxy	0.13 \pm 0.01
5c	3-Methoxy	0.93 \pm 0.41
5d	3-Methyl	0.83 \pm 0.36
5e	4-Chloro	0.34 \pm 0.16
5f	4-Bromo	0.45 \pm 0.23
5g	4-Nitro	0.39 \pm 0.20
5h	3-Nitro	0.13 \pm 0.01
5i	4-Aminosulfonyl	0.02 \pm 0.002
5j	3-Aminosulfonyl	0.12 \pm 0.04
5k	4-Carbamoyl	2.01 \pm 0.90
5l	4-Acetamido	0.65 \pm 0.35
6a	H	3.14 \pm 0.17
6b	4-Methoxy	1.33 \pm 0.11
6c	3-Methoxy	1.20 \pm 0.30
6d	3-Methyl	2.55 \pm 1.53
6e	4-Chloro	0.69 \pm 0.18
6f	4-Nitro	0.78 \pm 0.11
6g	3-Nitro	0.34 \pm 0.07
6h	4-Aminosulfonyl	0.26 \pm 0.01
6i	3-Aminosulfonyl	0.34 \pm 0.08
6j	4-Carbamoyl	1.22 \pm 0.23
6k	4-Acetamido	1.59 \pm 0.41
PP2 ^b		0.05 \pm 0.03

^a The inhibition rate (%) was calculated using the equation: $[1 - (A_{490}/A_{490}^{\text{control}})] \times 100\%$. IC_{50} values were obtained by Logit method based on the data obtained from three separate experiments; each compound concentration was tested in duplicate. % Inhibition rate at 10 μM .

^b PP2 was used as positive control.



Scheme 1. Reagents and conditions: (a) aniline (1.05 equiv.), *n*-pentanol, 70 °C, 5 h; (b) morpholine (5.0 equiv.), NaBF₄ (1.0 equiv.), DMSO, microwave, 5 min; (c) piperazine (5.0 equiv.), NaBF₄ (1.0 equiv.), DMSO, microwave, 5 min; (d) 2-(piperazin-1-yl)ethanol (5.0 equiv.), NaBF₄ (1.0 equiv.), DMSO, microwave, 5 min.

evaluated by the Ligandfit module of DS 2.1 (Forcefield: CHARMM; Pose Saving Maximum Poses Retained: 10). Conformational flexibility of the molecules from the library was considered in the docking search. Other parameters used in the DS 2.1 were default values. Three-hundred and eight molecules passed the druglikeness filter module were ranked by the scoring functions of Ligandfit, and analyzed for relatively lower binding energy, favorable shape complementarity, and potential in forming hydrogen bonds with Src kinase. In this way, 32 compounds (**4a–i**, **5a–l**, and **6a–k**) were finally selected for synthesis and bioassay (Fig. 4).

2.3. Chemical synthesis

On the basis of evaluation of binding potential and druglikeness, we selected 32 compounds (**4a–i**, **5a–l**, and **6a–k**) (Table 2) for synthesis and bioassay. Scheme 1 depicts the sequence of reactions that led to the preparation of desired products using 2,6-dichloropurine **2** as the starting material. In general, the 2-chloro-*N*-aromatic-9*H*-purin-6-amine **3** were prepared by 2,6-dichloropurine **2** through a nucleophilic addition reaction with anilines in *n*-pentanol. Subsequently, replacement of the C2 chloro by reacting with amines under microwave irradiation conditions in DMSO gave the targeted compounds **4a–i**, **5a–l**, and **6a–k**.

2.4. Tyrosine kinase assays

The tyrosine kinase activities of the purified proteins were determined in 96-well ELISA plates (Corning, NY) precoated with 20 µg/mL Poly(Glu,Tyr)_{4:1} (Sigma, St. Louis, MO). Briefly, 50 µL 10 µM ATP solution diluted in kinase reaction buffer (50 mM HEPES pH 7.4, 20 mM MgCl₂, 0.1 mM MnCl₂, 0.2 mM Na₃VO₄, 1 mM DTT) was added to each well. Then 10 µL of various concentrations of test compounds or reference compound dissolved in DMSO were added to each reaction well. The kinase reaction was performed in triplicate and initiated by adding tyrosine kinase diluted in 40 µL of kinase reaction buffer. After incubation at 37 °C for 60 min, the wells were washed three times with phosphate buffered saline (PBS) containing 0.1% Tween 20 (T-PBS). Next, 100 µL anti-phosphotyrosine (PY99) antibody (1:500, Santa Cruz Biotechnology, Santa Cruz, CA) diluted in T-PBS containing 5 mg/mL BSA was added and the plate was incubated at 37 °C for 30 min. After the plate was washed three times, 100 µL horseradish peroxidase-conjugated goat anti-mouse IgG (1:2000, Calbiochem, San Diego, CA) diluted in T-PBS containing 5 mg/mL BSA was added

and the plate was incubated at 37 °C for 30 min. The plate was washed, then 100 µL citrate buffer (0.1 M, pH 5.5) containing 0.03% H₂O₂ and 2 mg/mL *o*-phenylenediamine was added and samples were incubated at room temperature until color emerged. The reaction was terminated by adding 50 µL of 2 M H₂SO₄, and the plate was read using a multiwell spectrophotometer (VERSAmax™, Molecular Devices, Sunnyvale, CA, USA) at 492 nm. The inhibitory rate (%) was calculated with the formula: $[1 - (A_{492}/A_{492} \text{ control})] \times 100\%$. IC₅₀ values were calculated from the inhibitory curves.

2.5. Molecular docking simulation

To explore a more detail interaction mechanism between the most active compound and Src kinase, molecular docking simulation was carried out with the program AUTODOCK 4.0.1.³⁸ The three-dimensional (3D) structure of target protein of Src kinase is from Protein Data Bank (PDB entry No.: 1y57). The ligand and solvent molecules were removed from the crystal structure to obtain the docking grid and the active site was defined using AutoGrid. The grid size was set to 60 × 60 × 60 points with grid spacing of 0.375 Å. The grid box was centered on the center of the ligand from the corresponding crystal structure complexes. The Lamarckian genetic algorithm (LGA) is used for docking with the following settings: a maximum number of 1500,000 energy evaluations, an initial population of 50 randomly placed individuals, a maximum number of 37,000 generations, a mutation rate of 0.02, a crossover rate of 0.80 and an elitism value (number of top individuals that automatically survive) of 1. The ligand was fully optimized inside the binding site during the docking simulations. Finally, the conformation with the lowest predicted binding free energy of the most occurring binding modes in Src active pocket was selected.

3. Results and discussion

3.1. Focused library design and evaluation

In our preliminary study, we discovered two 2,6-disubstituted purine derivatives **1a** and **1b** exhibiting obvious Src kinase inhibitory activities, with IC₅₀s of 2.43 µM and 2.42 µM, respectively. Their chemical structures contain three parts: part A is a hydrophobic amines head, part B is a relatively hydrophilic alkyl tail, and framework is a linker between A and B (Fig. 2). To discover new chemical entities of Src kinase inhibitors with more potent

activities, a focused library was designed using the structural fragments isolated by the above and previously discovered inhibitors (15 fragments for part A, 8 fragments for part B, and 4 frameworks). Combining these fragments together, a $15 \times 8 \times 4$ focused library was obtained. Subsequently, the druglikeness of molecules from the combinatorial library was evaluated. Three-hundred and eight compounds which passed the filtration were picked out for further evaluation. Targeting the crystal structure of Src kinase, the focused library was then screened by using the scoring function of Ligandfit module that has been encoded in DS2.1. The docking results indicated that: (i) there is no significant difference between diverse amine substituents, but significant difference between amines and anilines substituents in part A; (ii) morpholine, piperazine, and 2-(piperazin-1-yl)ethanol substituents account for more than 70% in the top 50 molecules in part B; (iii) purine scaffold presents a dominant framework in the top 50 molecules. Accordingly, as the Src kinase inhibitors, the building blocks for parts B and the frameworks are fixed at morpholine, piperazine, 2-(piperazin-1-yl)ethanol, and purine. The fragment for part A is a little bit flexible. Considering the drug-like and docking screening analysis and synthetic feasibility, 32 compounds (**4a–i**, **5a–l**, and **6a–k**) were selected and synthesized for actual biological testing, and their chemical structures and bioassay results are listed in Table 1. These 32 compounds were synthesized through the routes outlined in Schemes 1, and the details for synthetic procedures and structural characterizations are described in Section 5.

3.2. Effectiveness of the approach

The hit rate of our design and screening approach is 100% regarding to binding. Of the 32 inhibitors, 18 compounds (**4e**, **4g**, **5a–j**, **5l**, and **6e–i**) showed potent activities in inhibiting the kinase activity of Src (Table 2), indicating that the hit rate with IC_{50} s against the enzymatic activity at submicromolar range is as high as 56.25%. The activity of the most potent one (Compound **5i**) improved by more than 120 times with an IC_{50} of 0.02 μ M. These results demonstrated that our approach not only enriched the hit rate of active compounds but also helped to discover new enzyme inhibitors with increased potency. Therefore, we might conclude that our approach, focused library construction combined with chemical synthesis and bioassay, is effective in discovering active compounds based on the 3D structure of a target.

3.3. Structure–activity relationships

Fragments for part A are structurally more diverse than fragments for part B. As part of a systematic SAR approach, we first investigated the importance of the alkyl side chains at 2-position (Table

2). Substitution studies revealed extremely similar results at this position. Morpholine analogs (**5a–l**) showed the best effect, and the activities of both the piperazine and 2-(piperazin-1-yl)ethanol analogs (**4a–i** and **6a–k**) decrease slightly. Our attention turned next to the modification of the substituents at the 6-position of the purine. Overall, substituents at both the *para*- and *meta*-positions on the amine ring are optimal for Src kinase inhibitory activity of these analogs. **1a** and **1b** exhibited moderate inhibition, with the IC_{50} values of 2.43 μ M and 2.42 μ M, respectively. No significant change was observed at the enzyme level when removing the substituents on 6-position amines (**5a** and **6a**). The methyl or methoxy substituent can be replaced with halogens, carbamoyl, and acetamido groups (**4b–c**, **4h–i**, **5e–f**, **5k–l**, **6e**, and **6j–k**) without loss of potency, while the substituents can be replaced with a nitro group (**4d–e**, **5g–h**, and **6f–g**) with minimal increase of potency. Introduction of a sulfonamide group (**4f–g**, **5i–j**, and **6h–i**) led to significant enhancement in potency. This improved enzyme potency could result from an increased donor and acceptor characters of the sulfonamide moiety binding the hinge region.

To explore the detailed binding characteristics of the compounds, the binding model of the most active compound **5i** with c-Src tyrosine kinase was constructed. Figure 5 shows the interaction model of **5i** to c-Src, indicating that it occupies the adenine pocket of the ATP-binding site, and locates at the hinge region through H-bonds with amino acid residues. The benzene sulfonamide head stretched deeply into the binding pocket with hydrophobic interaction, which was surrounded by residues Thr338, Lys295, and Asp404. The relatively hydrophilic alkyl tail appears to fit snugly at the entrance of the ATP-binding site. There are three H-bonds between **5i** and the hinge region of the Src kinase. 6-Position NH group forms two hydrogen bonds with the backbone carbonyl and NH of Met341, respectively, at the hinge region of the protein. The sulfonamide H atom forms an H-bond with the side-chain nitrogen of Thr338. The binding model of the representative compound highlights some of the critical H-bond interactions with the active site residues which were proved to be the key for kinase inhibitory activity. It may exert its tyrosine kinase inhibitory activity through the H-bonds to Met341 and Thr338, which are consistent with the previous reports.

3.4. Biological profile of compound 5i

3.4.1. Compound 5i selectively inhibits c-Src tyrosine kinase activity

To evaluate the selectivity profile, the most active inhibitor **5i** was tested in an enzymatic assay against a panel of 13 tyrosine kinases. The data confirmed the potency of **5i** against c-Src, and revealed **5i** was 100-fold and 300-fold less potent against Kit and

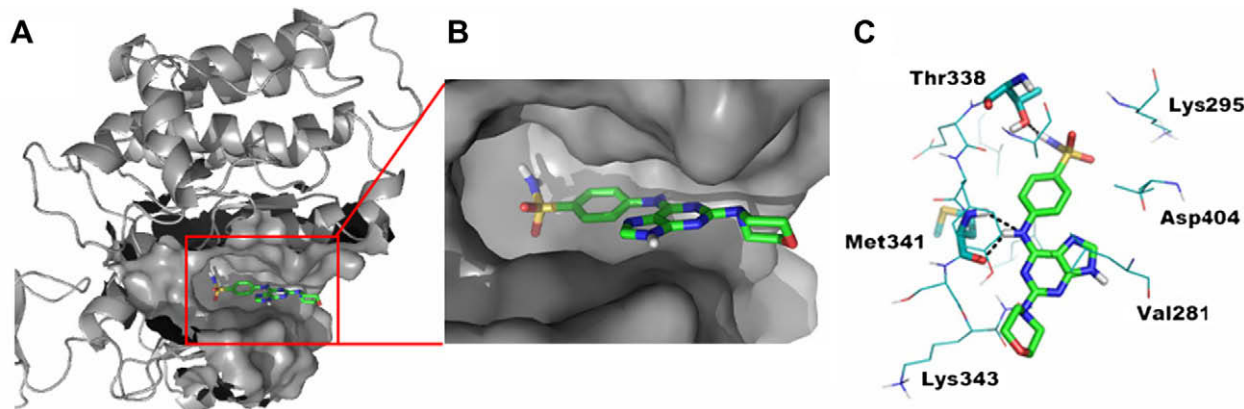


Figure 5. Binding model of compound **5i** in the binding cleft of Src kinase. The left part (A) and middle part (B) show the docking models of **5i** into the active sites of Src kinase. The right part (C) describes the detailed interactions between **5i** and Src kinase. These images were generated using the PYMOL program (<http://www.pymol.org>).

Table 3
Effects of **5i** on tyrosine kinase activities in cell-free system^a

Kinase	IC ₅₀ (μM)	% Inhibition at 10 μM ^b
Src	0.02 ± 0.002	97.8
c-Abl	6.00 ± 1.91	73.4
Kit	1.35 ± 0.15	83.1
EGFR	>10	18.5
ErbB2	>10	43.1
KDR	>10	47.2
VEGFR1	>10	0.0
PDGFRβ	>10	17.2
FGFR1	>10	48.7
FGFR2	>10	4.1
EphA2	>10	48.7
EphB2	>10	11.5
c-Met	>10	43.2

^a The inhibition rate (%) was calculated using the equation: $[1 - (A_{490}/A_{490} \text{ control})] \times 100\%$. IC₅₀ values were determined from three separate experiments; each compound concentration was tested in duplicate.

^b Values are means of three determinations and deviation from the means is <10% of the mean value.

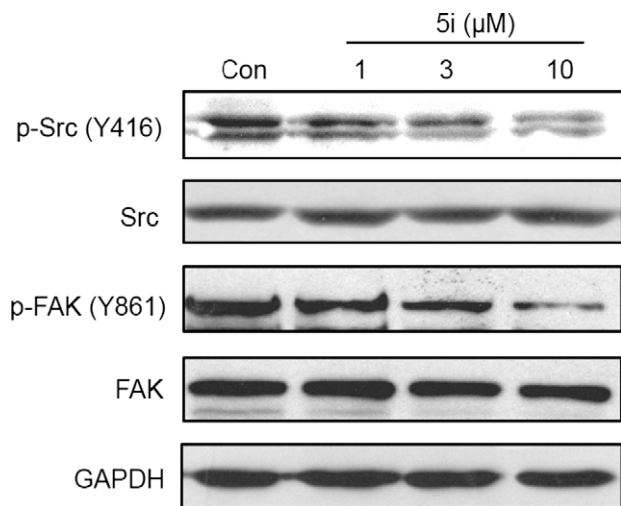


Figure 6. Effects of **5i** on the phosphorylation of c-Src and FAK in MDA-MB-231 cells. Data shown are representative of three independent Western blot assays.

c-Abl, respectively. Meanwhile, **5i** possessed weak inhibitory effect on EGFR, ErbB2, KDR, VEGFR1, KDR, PDGFR, FGFR1, FGFR2, EphA2, EphB2, and c-Met with IC₅₀ values above 10 μM (Table 3). These results indicate that **5i** is a highly selective inhibitor of c-Src kinase.

3.4.2. Compound **5i** abrogates phosphorylation of c-Src and FAK in cellular level

To explore the activity of **5i** on c-Src in intact cells, MDA-MB-231 human breast cancer cells that express high levels of c-Src were utilized. Exposure of MDA-MB-231 cells to **5i** resulted in down-regulation of phosphorylated c-Src and FAK, a substrate of c-Src, in a dose-dependent manner (Fig. 6), while the total protein levels of these two proteins remain unchanged after treatment with **5i**. These results indicated that **5i** inhibited c-Src activity in tumor cells.

3.4.3. Compound **5i** inhibits migration and invasion of MDA-MB-231 cells

As Src kinase is involved in regulating cell migration and invasion, we further investigated the effect of **5i** on these cellular processes. As shown in Figure 7A, cell migration was dramatically inhibited in a dose-dependent manner upon **5i** treatment, with a detectable inhibition at 3 μM and substantial inhibition at 10 μM. Similar results

were observed in the cell invasion assay (Fig. 7B). To exclude the inhibitory effects of **5i** on cell migration and invasion are due to its ability to inhibit cell proliferation, MTT assays were performed in MDA-MB-231 cells treated with the indicated concentrations of **5i** for 24 h. More than 95% of the cells were viable after **5i** treatment (data not shown). These findings revealed that the effects of **5i** on Src kinase activity resulted in decreased p-Src and p-FAK and contributed to inhibition of cell migration and invasion.

4. Conclusion

In summary, we discovered two 2,6-disubstituted purine derivatives **1a** and **1b** exhibiting obvious Src kinase inhibitory activity in the preliminary study. To discover novel entries of Src kinase inhibitors with more potent activity, a focused library containing 480 compounds was designed based on the chemical structures of the hits. Through druglikeness analysis and virtual screening, 32 compounds were selected from the focused library for chemical synthesis and bioassay. Remarkably, all of these compounds show Src kinase inhibitory activities, with IC₅₀ values ranging from 3.14 to 0.02 μM. The hit rate for inhibitors is 100%. The activity of the most potent one (**5i**) improved by more than 120 times than those of the hits. These data demonstrated that our approach could not only enrich the hit rate of active compounds but also help to discover new inhibitors with increased the potency. In addition, further study showed that **5i** exhibited highly selectivity for Src kinase among a panel of tyrosine kinases and inhibited phosphorylation of Src and its downstream signal transduction in MDA-MB-231 cells, which is accompanied with significant inhibition of cell migration and invasion. These results may provide insights into the discovery and development of novel 2,6-disubstituted purine derivatives with potent Src kinase inhibitory activities.

5. Experimental section

5.1. Chemistry

The reagents (chemicals) were purchased from commercial sources (Alfa, Acros, Sigma-Aldrich and Shanghai Chemical Reagent Company), and used without further purification. Analytical thin layer chromatography (TLC) was HSGF 254 (0.15–0.2 mm thickness, Yantai Huiyou Company, China). Yields were not optimized. Nuclear magnetic resonance (NMR) spectra were given on a AMX-300 (Bruker, Fällanden, Switzerland; internal standard as tetramethylsilane). Chemical shifts were reported in parts per million (ppm, δ) downfield from tetramethylsilane. Proton coupling patterns were described as singlet (s), doublet (d), triplet (t), quartet (q), multiplet (m), and broad (br). Low- and high-resolution (HRMS) mass spectra were given with an electric ionization and electrospray (EI, ESI) and a LCQ-DECA spectrometer produced by Finnigan MAT-95 (Finnigan, Santa Clara, CA, USA). Compounds **1c–k** were reported previously.³⁹ For the targeted compounds the chemical purity was determined using an Agilent 1100 Series HPLC. The purity of each compound was >95% (Table S1, Supplementary data).

5.1.1. General procedure for the synthesis of **1a–b**, **4a–i**, **5a–l**, and **6a–k**

To a stirred solution of 2,6-dichloro-purine (50 mmol) in 50 mL *n*-pentanol, aniline (52.5 mmol) was added at 70 °C. Stirring was continued until the precipitate was formed. Then the precipitate was filtered and washed with *n*-pentanol to give intermediate **3**. The crude product **3** (0.3 mmol) was dissolved in DMSO (4 mL) in a 10 mL glass vial equipped with a small magnetic stirring bar. To this was added 5 equiv amine and 5 equiv NaBF₄, and the vial

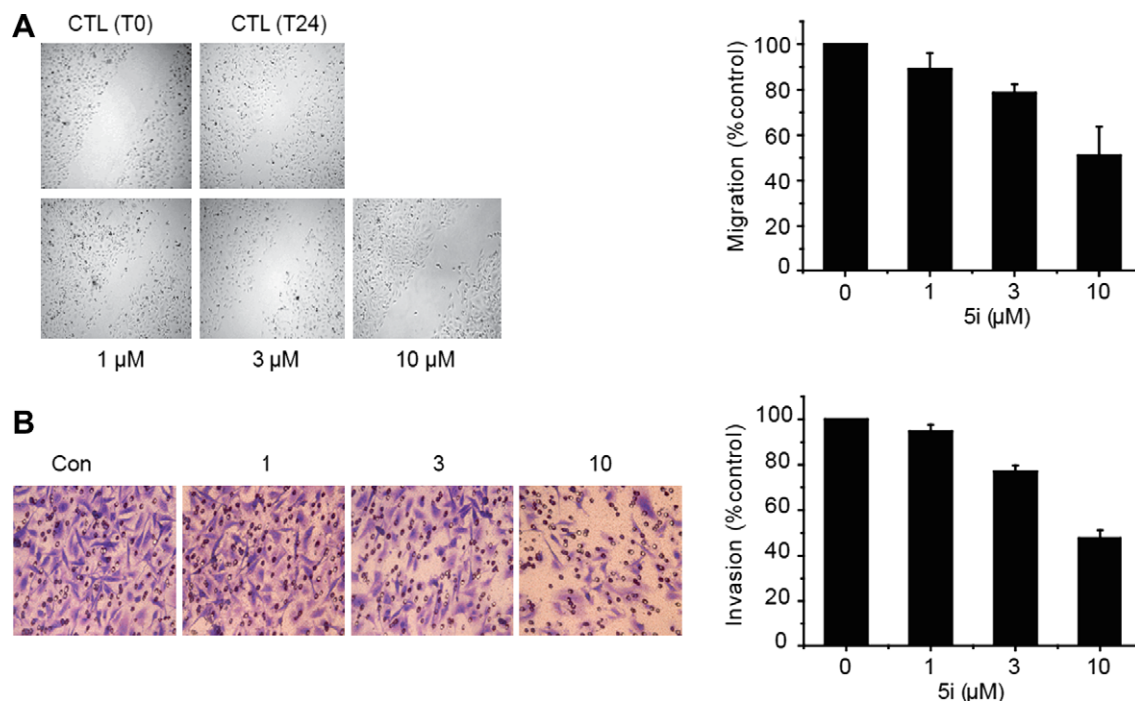


Figure 7. Compound **5i** suppresses MDA-MB-231 cell migration and invasion. (A) Compound **5i** inhibits cell migration. Wound-healing assay was applied to detect cell migration. MDA-MB-231 cells were treated with various concentrations of **5i** or vehicle for 24 h. Left, representative images of at least three independent experiments were presented. Right, quantification analysis of cell migration. Columns, mean of three experiments; bars, SD. (B) Compound **5i** inhibits cell invasion. Mitragel invasion chamber was used to detect cell invasion. MDA-MB-231 cells were treated with indicated concentrations of **5i** or vehicle. After 18 h, cells invading to the lower aspect of the Boyden chamber filter were stained and photographed. Left, representative images of at least three independent experiments were presented. Right, quantification analysis of cell invasion. Columns, mean of three experiments; bars, SD.

was tightly sealed with an aluminum/Teflon crimp top. The mixture was then irradiated for 5 min at 180 °C. After completion of the reaction, the vial was cooled to ambient temperature. Then water was added and the precipitated product was collected by filtrating. The resulting residuum was washed with water and purified by flash chromatography to give **1a–b**, **4a–i**, **5a–l**, and **6a–k**.

5.1.1.1. N-(4-Methoxyphenyl)-2-(piperazin-1-yl)-9H-purin-6-amine (1a). Prepared from 4-methoxyaniline and piperazine. Yield: 83%. Mp >250 °C; ¹H NMR (300 MHz, DMSO-*d*₆): δ 7.85 (s, 1H), 7.75 (d, *J* = 8.8 Hz, 2H), 6.90 (d, *J* = 8.8 Hz, 2H), 3.74 (s, 3H), 3.62–3.89 (m, 4H), 2.75–2.72 (m, 4H). MS (EI, *m/z*): 325 [M]⁺. HRMS (EI): calcd for C₁₆H₁₉N₇O [M]⁺, 325.1651, found 325.1642.

5.1.1.2. N-(3-Methylphenyl)-2-(piperazin-1-yl)-9H-purin-6-amine (1b). Prepared from 3-methylaniline and piperazine. Yield: 79%. Mp >250 °C; ¹H NMR (300 MHz, DMSO-*d*₆): δ 7.88 (s, 1H), 7.79 (s, 1H), 7.61 (d, *J* = 8.0 Hz, 1H), 7.19 (t, *J* = 8.0 Hz, 1H), 6.82 (d, *J* = 8.0 Hz, 1H), 3.66–3.63 (m, 4H), 2.78–2.75 (m, 4H), 2.29 (s, 3H). MS (EI, *m/z*): 309 [M]⁺. HRMS (EI): calcd for C₁₆H₁₉N₇ [M]⁺, 309.1702, found 309.1693.

5.1.1.3. N-(3-Methoxyphenyl)-2-(piperazin-1-yl)-9H-purin-6-amine (4a). Prepared from 3-methoxyaniline and piperazine. Yield: 84%. Mp 189–191 °C; ¹H NMR (300 MHz, DMSO-*d*₆): δ 7.89 (s, 1H), 7.67 (s, 1H), 7.38 (d, *J* = 8.0 Hz, 1H), 7.20 (t, *J* = 8.0 Hz, 1H), 6.57 (d, *J* = 8.0 Hz, 1H), 3.75 (s, 3H), 3.68–3.63 (m, 4H), 2.79–2.73 (m, 4H). MS (EI, *m/z*): 325 [M]⁺. HRMS (EI): calcd for C₁₆H₁₉N₇O [M]⁺, 325.1651, found 325.1643.

5.1.1.4. N-(4-Chlorophenyl)-2-(piperazin-1-yl)-9H-purin-6-amine (4b). Prepared from 4-chloroaniline and piperazine. Yield: 87%. Mp >250 °C; ¹H NMR (300 MHz, DMSO-*d*₆): δ 7.90 (d, *J* = 8.8 Hz, 2H), 7.89 (s, 1H), 7.36 (d, *J* = 8.8 Hz, 2H), 3.65–3.60 (m,

4H), 2.80–2.74 (m, 4H). MS (EI, *m/z*): 329 [M]⁺. HRMS (EI): calcd for C₁₅H₁₆ClN₇ [M]⁺, 329.1156, found 329.1145.

5.1.1.5. N-(4-Bromophenyl)-2-(piperazin-1-yl)-9H-purin-6-amine (4c). Prepared from 4-bromoaniline and piperazine. Yield: 80%. Mp >250 °C; ¹H NMR (300 MHz, DMSO-*d*₆): δ 7.90 (s, 1H), 7.85 (d, *J* = 9.0 Hz, 2H), 7.48 (d, *J* = 9.0 Hz, 2H), 3.65–3.60 (m, 4H), 2.80–2.74 (m, 4H). MS (EI, *m/z*): 373 [M]⁺. HRMS (EI): calcd for C₁₅H₁₆BrN₇ [M]⁺, 373.0651, found 373.0647.

5.1.1.6. N-(4-Nitroxyphenyl)-2-(piperazin-1-yl)-9H-purin-6-amine (4d). Prepared from 4-nitroaniline and piperazine. Yield: 76%. Mp >250 °C; ¹H NMR (300 MHz, DMSO-*d*₆): δ 8.20 (q, *J* = 9.6 Hz, 4H), 7.99 (s, 1H), 3.71–3.67 (m, 4H), 2.87–2.82 (m, 4H). MS (EI, *m/z*): 340 [M]⁺. HRMS (EI): calcd for C₁₅H₁₆N₈O₂ [M]⁺, 340.1396, found 340.1392.

5.1.1.7. N-(3-Nitroxyphenyl)-2-(piperazin-1-yl)-9H-purin-6-amine (4e). Prepared from 3-nitroaniline and piperazine. Yield: 78%. Mp >250 °C; ¹H NMR (300 MHz, DMSO-*d*₆): δ 8.10 (d, *J* = 8.0 Hz, 1H), 7.95 (s, 1H), 7.87 (s, 1H), 7.82 (d, *J* = 8.0 Hz, 1H), 7.58 (t, *J* = 8.0 Hz, 1H), 3.74–3.65 (m, 4H), 2.84–2.76 (m, 4H). MS (EI, *m/z*): 340 [M]⁺. HRMS (EI): calcd for C₁₅H₁₆N₈O₂ [M]⁺, 340.1396, found 340.1390.

5.1.1.8. N-(4-Aminosulfonylphenyl)-2-(piperazin-1-yl)-9H-purin-6-amine (4f). Prepared from 4-aminobenzenesulfonamide and piperazine. Yield: 71%. Mp 219–221 °C; ¹H NMR (300 MHz, DMSO-*d*₆): δ 8.05 (d, *J* = 8.7 Hz, 2H), 7.95 (s, 1H), 7.76 (d, *J* = 8.7 Hz, 2H), 3.75–3.68 (m, 4H), 2.44–2.37 (m, 4H). MS (EI, *m/z*): 374 [M]⁺. HRMS (EI): calcd for C₁₅H₁₈N₈O₂S [M]⁺, 374.1273, found 374.1262.

5.1.1.9. N-(3-Aminosulfonylphenyl)-2-(piperazin-1-yl)-9H-purin-6-amine (4g). Prepared from 3-aminobenzenesulfonamide and piperazine. Yield: 71%. Mp 219–221 °C; ¹H NMR (300 MHz, DMSO-*d*₆): δ 8.05 (d, *J* = 8.7 Hz, 2H), 7.95 (s, 1H), 7.76 (d, *J* = 8.7 Hz, 2H), 3.75–3.68 (m, 4H), 2.44–2.37 (m, 4H). MS (EI, *m/z*): 374 [M]⁺. HRMS (EI): calcd for C₁₅H₁₈N₈O₂S [M]⁺, 374.1273, found 374.1262.

mide and piperazine. Yield: 65%. Mp >250 °C; ¹H NMR (300 MHz, DMSO-*d*₆): δ 7.93 (s, 1H), 7.83 (d, *J* = 7.7 Hz, 1H), 7.52–7.42 (m, 2H), 7.29 (s, 1H), 3.72–3.63 (m, 4H), 2.82–2.74 (m, 4H). MS (EI, *m/z*): 374 [M]⁺. HRMS (EI): calcd for C₁₅H₁₈N₈O₂S [M]⁺, 374.1273, found 374.1263.

5.1.1.10. *N*-(4-Carbamoylphenyl)-2-(piperazin-1-yl)-9H-purin-6-amine (4h). Prepared from 4-carbamoylaniline and piperazine. Yield: 63%. Mp >250 °C; ¹H NMR (300 MHz, DMSO-*d*₆): δ 7.97 (d, *J* = 8.6 Hz, 2H), 7.93 (s, 1H), 7.85 (d, *J* = 8.6 Hz, 2H), 3.68–3.61 (m, 4H), 2.80–2.74 (m, 4H). MS (EI, *m/z*): 338 [M]⁺. HRMS (EI): calcd for C₁₆H₁₈N₈O [M]⁺, 338.1604, found 338.1588.

5.1.1.11. *N*-(4-Acetamidophenyl)-2-(piperazin-1-yl)-9H-purin-6-amine (4i). Prepared from 4-acetamidoaniline and piperazine. Mp >250 °C; Yield: 69%. ¹H NMR (300 MHz, DMSO-*d*₆): δ 8.16 (s, 1H), 8.07 (d, *J* = 8.7 Hz, 2H), 7.80 (d, *J* = 8.7 Hz, 2H), 3.91 (br s, 4H), 3.06 (br s, 4H), 2.33 (s, 3H). MS (EI, *m/z*): 352 [M]⁺. HRMS (EI): calcd for C₁₇H₂₀N₈O [M]⁺, 352.1760, found 352.1762.

5.1.1.12. *N*-phenyl-2-morpholino-9H-purin-6-amine (5a). Prepared from aniline and morpholine. Yield: 80%. Mp >250 °C; ¹H NMR (300 MHz, DMSO-*d*₆): δ 7.94 (s, 1H), 7.87 (d, *J* = 8.0 Hz, 2H), 7.32 (t, *J* = 8.0 Hz, 2H), 7.00 (t, *J* = 8.0 Hz, 1H), 3.71–3.62 (m, 8H). MS (EI, *m/z*): 296 [M]⁺. HRMS (EI): calcd for C₁₅H₁₆N₆O [M]⁺, 296.1386, found 296.1391.

5.1.1.13. *N*-(4-Methoxyphenyl)-2-morpholino-9H-purin-6-amine (5b). Prepared from 4-methoxyaniline and morpholine. Yield: 84%. Mp 244–246 °C; ¹H NMR (300 MHz, CDCl₃): δ 7.60 (d, *J* = 8.8 Hz, 2H), 7.50 (s, 1H), 6.90 (d, *J* = 8.8 Hz, 2H), 3.76 (s, 3H), 3.72–3.65 (m, 8H). MS (EI, *m/z*): 326 [M]⁺. HRMS (EI): calcd for C₁₆H₁₈N₆O₂ [M]⁺, 326.1491, found 326.1481.

5.1.1.14. *N*-(3-Methoxyphenyl)-2-morpholino-9H-purin-6-amine (5c). Prepared from 3-methoxyaniline and morpholine. Yield: 88%. Mp 242–243 °C; ¹H NMR (300 MHz, DMSO-*d*₆): δ 7.91 (s, 1H), 7.65 (s, 1H), 7.42 (d, *J* = 8.0 Hz, 1H), 7.20 (t, *J* = 8.0 Hz, 1H), 6.57 (d, *J* = 8.0 Hz, 1H), 3.74 (s, 3H), 3.69–3.65 (m, 8H). MS (EI, *m/z*): 326 [M]⁺. HRMS (EI): calcd for C₁₆H₁₈N₆O₂ [M]⁺, 326.1491, found 326.1496.

5.1.1.15. *N*-(3-Methylphenyl)-2-morpholino-9H-purin-6-amine (5d). Prepared from 3-methylaniline and morpholine. Yield: 81%. Mp 238–240 °C; ¹H NMR (300 MHz, DMSO-*d*₆): δ 7.90 (s, 1H), 7.77 (s, 1H), 7.63 (d, *J* = 8.0 Hz, 1H), 7.19 (t, *J* = 8.0 Hz, 1H), 6.82 (d, *J* = 8.0 Hz, 1H), 3.71–3.63 (m, 8H), 2.29 (s, 3H). MS (EI, *m/z*): 310 [M]⁺. HRMS (EI): calcd for C₁₆H₁₈N₆O [M]⁺, 310.1542, found 310.1538.

5.1.1.16. *N*-(4-Chlorophenyl)-2-morpholino-9H-purin-6-amine (5e). Prepared from 4-chloroaniline and morpholine. Yield: 79%. Mp >250 °C; ¹H NMR (300 MHz, DMSO-*d*₆): δ 7.92 (s, 1H), 7.90 (d, *J* = 8.8 Hz, 2H), 7.36 (d, *J* = 8.8 Hz, 2H), 3.70–3.61 (m, 8H). MS (EI, *m/z*): 330 [M]⁺. HRMS (EI): calcd for C₁₅H₁₅ClN₆O [M]⁺, 330.0996, found 330.0995.

5.1.1.17. *N*-(4-Bromophenyl)-2-morpholino-9H-purin-6-amine (5f). Prepared from 4-bromoaniline and morpholine. Yield: 84%. Mp >250 °C; ¹H NMR (300 MHz, DMSO-*d*₆): δ 7.93 (s, 1H), 7.86 (d, *J* = 8.8 Hz, 2H), 7.49 (d, *J* = 8.8 Hz, 2H), 3.73–3.58 (m, 8H). MS (EI, *m/z*): 374 [M]⁺. HRMS (EI): calcd for C₁₅H₁₅BrN₆O [M]⁺, 374.0491, found 374.0479.

5.1.1.18. *N*-(4-Nitrophenyl)-2-morpholino-9H-purin-6-amine (5g). Prepared from 4-nitroaniline and morpholine. Yield: 83%.

Mp >250 °C; ¹H NMR (300 MHz, DMSO-*d*₆): δ 8.21 (q, *J* = 9.5 Hz, 4H), 8.01 (s, 1H), 3.73–3.65 (m, 8H). MS (EI, *m/z*): 341 [M]⁺. HRMS (EI): calcd for C₁₅H₁₅N₇O₃ [M]⁺, 341.1236, found 341.1232.

5.1.1.19. *N*-(3-Nitrophenyl)-2-morpholino-9H-purin-6-amine (5h). Prepared from 3-nitroaniline and morpholine. Yield: 80%. Mp >250 °C; ¹H NMR (300 MHz, DMSO-*d*₆): δ 8.12 (d, *J* = 8.0 Hz, 1H), 8.01 (s, 1H), 7.91 (s, 1H), 7.83 (d, *J* = 8.0 Hz, 1H), 7.58 (t, *J* = 8.0 Hz, 1H), 3.72 (br s, 8H). MS (EI, *m/z*): 341 [M]⁺. HRMS (EI): calcd for C₁₅H₁₅N₇O₃ [M]⁺, 341.1236, found 341.1231.

5.1.1.20. *N*-(4-Aminosulfonylphenyl)-2-morpholino-9H-purin-6-amine (5i). Prepared from 4-aminobenzenesulfonamide and morpholine. Yield: 76%. Mp >250 °C; ¹H NMR (300 MHz, DMSO-*d*₆): δ 8.06 (d, *J* = 8.8 Hz, 2H), 7.96 (s, 1H), 7.76 (d, *J* = 8.8 Hz, 2H), 3.73–3.63 (m, 8H). MS (EI, *m/z*): 375 [M]⁺. HRMS (EI): calcd for C₁₅H₁₇N₇O₃S [M]⁺, 375.1114, found 375.1101.

5.1.1.21. *N*-(3-Aminosulfonylphenyl)-2-morpholino-9H-purin-6-amine (5j). Prepared from 3-aminobenzenesulfonamide and morpholine. Yield: 76%. Mp >250 °C; ¹H NMR (300 MHz, DMSO-*d*₆): δ 7.96 (s, 1H), 7.82 (d, *J* = 7.7 Hz, 1H), 7.51–7.43 (m, 2H), 7.29 (s, 1H), 3.71–3.65 (m, 8H). MS (EI, *m/z*): 375 [M]⁺. HRMS (EI): calcd for C₁₅H₁₇N₇O₃S [M]⁺, 375.1114, found 375.1110.

5.1.1.22. *N*-(4-Carbamoylphenyl)-2-morpholino-9H-purin-6-amine (5k). Prepared from 4-carbamoylaniline and morpholine. Yield: 69%. Mp >250 °C; ¹H NMR (300 MHz, DMSO-*d*₆): δ 7.97 (d, *J* = 8.4 Hz, 2H), 7.90 (s, 1H), 7.85 (d, *J* = 8.4 Hz, 2H), 3.73–3.64 (m, 8H). MS (EI, *m/z*): 339 [M]⁺. HRMS (EI): calcd for C₁₆H₁₇N₇O₂ [M]⁺, 339.1444, found 339.1437.

5.1.1.23. *N*-(4-Acetamidophenyl)-2-morpholino-9H-purin-6-amine (5l). Prepared from 4-acetamidoaniline and morpholine. Yield: 66%. Mp >250 °C; ¹H NMR (300 MHz, DMSO-*d*₆): δ 7.88 (s, 1H), 7.78–7.71 (m, 2H), 7.56–7.49 (m, 2H), 3.72–3.58 (m, 8H), 2.03 (s, 3H). MS (EI, *m/z*): 353 [M]⁺. HRMS (EI): calcd for C₁₇H₁₉N₇O₂ [M]⁺, 353.1600, found 353.1591.

5.1.1.24. *N*-Phenyl-2-(4-(2-hydroxyethyl)piperazin-1-yl)-9H-purin-6-amine (6a). Prepared from aniline and 2-(piperazin-1-yl)ethanol. Yield: 74%. Mp >250 °C; ¹H NMR (300 MHz, DMSO-*d*₆): δ 7.88 (s, 1H), 7.87–7.85 (m, 2H), 7.29 (t, *J* = 8.4 Hz, 2H), 6.97 (t, *J* = 8.4 Hz, 1H), 3.70–3.62 (m, 4H), 3.53 (t, *J* = 6.2 Hz, 1H), 2.48–2.45 (m, 4H), 2.41 (t, *J* = 6.2 Hz, 1H). MS (EI, *m/z*): 339 [M]⁺. HRMS (EI): calcd for C₁₇H₂₁N₇O [M]⁺, 339.1808, found 339.1802.

5.1.1.25. *N*-(4-Methoxyphenyl)-2-(4-(2-hydroxyethyl)piperazin-1-yl)-9H-purin-6-amine (6b). Prepared from 4-methoxyaniline and 2-(piperazin-1-yl)ethanol. Yield: 81%. Mp 240–241 °C; ¹H NMR (300 MHz, DMSO-*d*₆): δ 7.83 (s, 1H), 7.75 (d, *J* = 9.0 Hz, 2H), 6.88 (d, *J* = 9.0 Hz, 2H), 3.73 (s, 3H), 3.68–3.62 (m, 4H), 3.54 (t, *J* = 6.0 Hz, 2H), 2.50–2.45 (m, 4H), 2.42 (t, *J* = 6.0 Hz, 2H). MS (EI, *m/z*): 369 [M]⁺. HRMS (EI): calcd for C₁₈H₂₃N₇O₂ [M]⁺, 369.1913, found 369.1908.

5.1.1.26. *N*-(3-Methoxyphenyl)-2-(4-(2-hydroxyethyl)piperazin-1-yl)-9H-purin-6-amine (6c). Prepared from 3-methoxyaniline and 2-(piperazin-1-yl)ethanol. Yield: 75%. Mp 226–227 °C; ¹H NMR (300 MHz, DMSO-*d*₆): δ 7.88 (s, 1H), 7.70–7.68 (m, 1H), 7.40 (d, *J* = 8.0 Hz, 1H), 7.18 (t, *J* = 8.0 Hz, 1H), 6.54 (dd, *J* = 8.0 Hz, 2.3 Hz, 1H), 3.74 (s, 3H), 3.70–3.66 (m, 4H), 3.53 (t, *J* = 6.2 Hz, 2H), 2.49–2.44 (m, 4H), 2.41 (t, *J* = 6.2 Hz, 2H). MS (EI, *m/z*): 369 [M]⁺. HRMS (EI): calcd for C₁₈H₂₃N₇O₂ [M]⁺, 369.1913, found 369.1917.

5.1.1.27. *N*-(3-Methylphenyl)-2-(4-(2-hydroxyethyl)piperazin-1-yl)-9*H*-purin-6-amine (6d). Prepared from 3-methylaniline and 2-(piperazin-1-yl)ethanol. Yield: 80%. Mp >250 °C; ¹H NMR (300 MHz, DMSO-*d*₆): δ 7.86 (s, 1H), 7.82 (s, 1H), 7.60 (d, *J* = 8.0 Hz, 1H), 7.16 (t, *J* = 8.0 Hz, 1H), 6.79 (d, *J* = 8.0 Hz, 1H), 3.71–3.64 (m, 4H), 3.53 (t, *J* = 6.2 Hz, 2H), 2.50–2.45 (m, 4H), 2.41 (t, *J* = 6.2 Hz, 2H), 2.28 (s, 3H). MS (EI, *m/z*): 353 [M]⁺. HRMS (EI): calcd for C₁₈H₂₃N₇O [M]⁺, 353.1964, found 353.1963.

5.1.1.28. *N*-(4-Chlorophenyl)-2-(4-(2-hydroxyethyl)piperazin-1-yl)-9*H*-purin-6-amine (6e). Prepared from 4-chloroaniline and 2-(piperazin-1-yl)ethanol. Yield: 79%. Mp >250 °C; ¹H NMR (300 MHz, DMSO-*d*₆): δ 7.91 (d, *J* = 8.6 Hz, 2H), 7.89 (s, 1H), 7.34 (d, *J* = 8.6 Hz, 2H), 3.69–3.62 (m, 4H), 3.53 (t, *J* = 6.2 Hz, 2H), 2.49–2.44 (m, 4H), 2.41 (t, *J* = 6.2 Hz, 2H). MS (EI, *m/z*): 373 [M]⁺. HRMS (EI): calcd for C₁₇H₂₀ClN₇O [M]⁺, 373.1418, found 373.1409.

5.1.1.29. *N*-(4-Nitrophenyl)-2-(4-(2-hydroxyethyl)piperazin-1-yl)-9*H*-purin-6-amine (6f). Prepared from 4-nitroaniline and 2-(piperazin-1-yl)ethanol. Yield: 75%. Mp >250 °C; ¹H NMR (300 MHz, DMSO-*d*₆): δ 8.19 (q, *J* = 9.0 Hz, 4H), 7.98 (s, 1H), 3.72–3.66 (m, 4H), 3.54 (t, *J* = 6.2 Hz, 2H), 2.54–2.49 (m, 4H), 2.42 (t, *J* = 6.2 Hz, 2H). MS (EI, *m/z*): 384 [M]⁺. HRMS (EI): calcd for C₁₇H₂₀N₈O₃ [M]⁺, 384.1658, found 384.1648.

5.1.1.30. *N*-(3-Nitrophenyl)-2-(4-(2-hydroxyethyl)piperazin-1-yl)-9*H*-purin-6-amine (6g). Prepared from 3-nitroaniline and 2-(piperazin-1-yl)ethanol. Yield: 80%. Mp >250 °C; ¹H NMR (300 MHz, DMSO-*d*₆): δ 8.11 (d, *J* = 8.1 Hz, 1H), 7.96 (s, 1H), 7.88 (s, 1H), 7.83 (d, *J* = 8.1 Hz, 1H), 7.58 (d, *J* = 8.1 Hz, 1H), 3.79–3.72 (m, 4H), 3.35 (t, *J* = 5.9 Hz, 2H), 2.57–2.51 (m, 4H), 2.46 (t, *J* = 5.9 Hz, 2H). MS (EI, *m/z*): 384 [M]⁺. HRMS (EI): calcd for C₁₇H₂₀N₈O₃ [M]⁺, 384.1658, found 384.1648.

5.1.1.31. *N*-(4-Aminosulfonylphenyl)-2-(4-(2-hydroxyethyl)piperazin-1-yl)-9*H*-purin-6-amine (6h). Prepared from 4-amino-benzenesulfonamide and 2-(piperazin-1-yl)ethanol. Yield: 62%. Mp >250 °C; ¹H NMR (300 MHz, DMSO-*d*₆): δ 8.05 (d, *J* = 8.8 Hz, 1H), 7.95 (s, 1H), 7.76 (d, *J* = 8.8 Hz, 1H), 3.74–3.66 (m, 4H), 3.52 (t, *J* = 6.2 Hz, 2H), 2.52–2.48 (m, 4H), 2.45 (t, *J* = 6.2 Hz, 2H). MS (EI, *m/z*): 418 [M]⁺. HRMS (EI): calcd for C₁₇H₂₂N₈O₃S [M]⁺, 418.1536, found 418.1533.

5.1.1.32. *N*-(3-Aminosulfonylphenyl)-2-(4-(2-hydroxyethyl)piperazin-1-yl)-9*H*-purin-6-amine (6i). Prepared from 3-amino-benzenesulfonamide and 2-(piperazin-1-yl)ethanol. Yield: 66%. Mp >250 °C; ¹H NMR (300 MHz, DMSO-*d*₆): δ 7.93 (s, 1H), 7.82 (d, *J* = 8.1 Hz, 1H), 7.51–7.42 (m, 2H), 7.28 (s, 1H), 3.74–3.68 (m, 4H), 3.55 (t, *J* = 6.2 Hz, 2H), 2.50–2.46 (m, 4H), 2.44 (t, *J* = 6.2 Hz, 2H). MS (EI, *m/z*): 418 [M]⁺. HRMS (EI): calcd for C₁₇H₂₂N₈O₃S [M]⁺, 418.1536, found 418.1526.

5.1.1.33. *N*-(4-Carbamoylphenyl)-2-(4-(2-hydroxyethyl)piperazin-1-yl)-9*H*-purin-6-amine (6j). Prepared from 4-carbamoylaniline and 2-(piperazin-1-yl)ethanol. Yield: 47%. Mp >250 °C; ¹H NMR (300 MHz, DMSO-*d*₆): δ 7.98 (d, *J* = 8.6 Hz, 2H), 7.92 (s, 1H), 7.84 (d, *J* = 8.6 Hz, 2H), 3.75–3.66 (m, 4H), 3.54 (t, *J* = 6.2 Hz, 2H), 2.54–2.51 (m, 4H), 2.44 (t, *J* = 6.2 Hz, 2H). MS (EI, *m/z*): 382 [M]⁺. HRMS (EI): calcd for C₁₈H₂₂N₈O₂ [M]⁺, 382.1866, found 382.1866.

5.1.1.34. *N*-(4-Acetamidophenyl)-2-(4-(2-hydroxyethyl)piperazin-1-yl)-9*H*-purin-6-amine (6k). Prepared from 4-acetamidoaniline and 2-(piperazin-1-yl)ethanol. Yield: 58%. Mp >250 °C; ¹H NMR (300 MHz, DMSO-*d*₆): δ 7.86 (s, 1H), 7.77 (d, *J* = 8.8 Hz, 2H), 7.50 (d, *J* = 8.8 Hz, 2H), 3.72–3.63 (m, 4H), 3.55 (t,

J = 6.3 Hz, 2H), 2.50–2.45 (m, 4H), 2.42 (t, *J* = 6.3 Hz, 2H), 2.04 (s, 3H). MS (EI, *m/z*): 396 [M]⁺. HRMS (EI): calcd for C₁₉H₂₄N₈O₂ [M]⁺, 396.2022, found 396.2026.

5.2. Pharmacology

5.2.1. Materials

The kinase domain of tyrosine kinase c-Src, epidermal growth factor receptor 1 (EGFR/ErbB-1), epidermal growth factor receptor 2 (EGFR-2/ErbB-2), vascular endothelial growth factor receptor 2 (VEGFR-2/KDR), stem cell factor receptor c-kit, fibroblast growth factor receptor-1 and -2 (FGFR-1, FGFR-2), EphA2, EphB2, and c-Met were expressed using the Bac-to-Bac baculovirus expression system (Invitrogen, Carlsbad, CA) and purified on Ni-NTA columns (QIAGEN Inc., Valencia, CA) as previously described. Vascular endothelial growth factor receptor 1 (VEGFR-1/Flt-1), platelet derived growth factor receptorβ (PDGFRβ) and c-Abl kinase were purchased from Upstate Biotechnology Inc. (Charlottesville, VA).

5.2.2. Cells lines and cell culture

MDA-MB-231 human breast cancer cells were obtained from American Type Culture Collection and cultured in Leibovitz's L15 Medium supplemented with 10% fetal bovine serum, 100 units/mL penicillin sodium and 100 μg/mL streptomycin sulfate. Cells were cultured in a humidified atmosphere of 5% CO₂ and 95% air at 37 °C.

5.2.3. Western blot analysis

Cells (4.5 × 10⁵) were plated in six-well plate overnight, and then exposed to **5i** at concentrations of 1, 3, and 10 μM, or DMSO alone, for 24 h. Western blot analyses were subsequently performed with standard procedures. Antibodies against the following were used: p-Src (Tyr416) (#2113) (Cell Signaling Technologies, Cambridge, MA), Src(sc-19), FAK(sc-557), and GAPDH(sc-47724) were obtained from (Santa Cruz Biotechnology, Santa Cruz, CA), p-FAK (Tyr861) (44-626G) (BioSource International, Camarillo, CA).

5.2.4. Wound-healing assay

Cells were plated in 24-well tissue culture plates, grown to confluent. Monolayer wounds were produced using a pipette tip scratched through the center of the well. Medium and non-adherent cells were aspirated, the adherent cells were washed once, and new medium containing various concentrations of **5i**, or DMSO alone, was added. Photographs of the initial wound were taken for comparison. After incubation for 24 h, photographs of the same scraped section were taken. Distances of denuded areas were measured and compared with time 0.

5.2.5. Cell invasion assay

Transwell chamber membranes (6.5 mm diameter, 8 μm pore size; Costar, Corning, NY) were coated with 100 μL of 1 mg/mL Matrigel (dissolved in serum-free L15 medium; Becton Dickinson Sciences, Franklin Lakes, NJ). 10% FBS were added to lower chambers. Cells and various concentrations of compound, or DMSO alone, were added to the upper chambers at the same time and allowed to invade for 18 h at 37 °C. Cells that had not invaded were removed from the upper chamber with a cotton swab. The remaining cells were fixed, stained with 0.1% crystal violet, and photographs were taken under a microscope and measured at 595 nm after extraction with 10% acetic acid for 10 min.

Acknowledgments

We gratefully acknowledge financial support from the State Key Program of Basic Research of China (Grant 2002CB512802), the National Natural Science Foundation of China (Grants 20372069, 29725203, 20721003 and 20872153), the 863 Hi-Tech Program of China (Grants 2006AA020602 and 2006AA020402), National

S&T Major Projects (2009ZX09301-001, 2009ZX09501-001 and 2009ZX09501-010).

Supplementary data

Supplementary data associated with this article can be found, in the online version, at doi:10.1016/j.bmc.2010.05.032.

References and notes

- Martin, G. S. *Nat. Rev. Mol. Cell Biol.* **2001**, *2*, 467.
- Yeatman, T. J. *Nat. Rev. Cancer* **2004**, *4*, 470.
- Finn, R. S. *Ann. Oncol.* **2008**, *19*, 1379.
- Summy, J. M.; Gallick, G. E. *Cancer Metastasis Rev.* **2003**, *22*, 337.
- Frame, M. C. *Biochim. Biophys. Acta* **2002**, *1602*, 114.
- Summy, J. M.; Gallick, G. E. *Clin. Cancer Res.* **2006**, *12*, 1398.
- Rucci, N.; Susa, M.; Teti, A. *Anticancer Agents Med. Chem.* **2008**, *8*, 342.
- Hilbig, A. *Recent Results Cancer Res.* **2008**, *177*, 179.
- Boyce, B. F.; Xing, L.; Yao, Z.; Yamashita, T.; Shakespeare, W. C.; Wang, Y.; Metcalf, C. A., III; Sundaramoorthi, R.; Dalgarno, D. C.; Iuliucci, J. D.; Sawyer, T. K. *Clin. Cancer Res.* **2006**, *12*, 6291s.
- Park, S. I.; Zhang, J.; Phillips, K. A.; Araujo, J. C.; Najjar, A. M.; Volgin, A. Y.; Gelovani, J. G.; Kim, S. J.; Wang, Z.; Gallick, G. E. *Cancer Res.* **2008**, *68*, 3323.
- Lombardo, L. J.; Lee, F. Y.; Chen, P.; Norris, D.; Barrish, J. C.; Behnia, K.; Castaneda, S.; Cornelius, L. A.; Das, J.; Doweiko, A. M.; Fairchild, C.; Hunt, J. T.; Inigo, I.; Johnston, K.; Kamath, A.; Kan, D.; Klei, H.; Marathe, P.; Pang, S.; Peterson, R.; Pitt, S.; Schieven, G. L.; Schmidt, R. J.; Tokarski, J.; Wen, M. L.; Wityak, J.; Borzilleri, R. M. *J. Med. Chem.* **2004**, *47*, 6658.
- Das, J.; Chen, P.; Norris, D.; Padmanabha, R.; Lin, J.; Moquin, R. V.; Shen, Z.; Cook, L. S.; Doweiko, A. M.; Pitt, S.; Pang, S.; Shen, D. R.; Fang, Q.; de Fex, H. F.; McIntyre, K. W.; Shuster, D. J.; Gillooly, K. M.; Behnia, K.; Schieven, G. L.; Wityak, J.; Barrish, J. C. *J. Med. Chem.* **2006**, *49*, 6819.
- Serrels, B.; Serrels, A.; Mason, S. M.; Baldeschi, C.; Ashton, G. H.; Canel, M.; Mackintosh, L. J.; Doyle, B.; Green, T. P.; Frame, M. C.; Sansom, O. J.; Brunton, V. G. *Carcinogenesis* **2009**, *30*, 249.
- Huang, W. S.; Zhu, X.; Wang, Y.; Azam, M.; Wen, D.; Sundaramoorthi, R.; Thomas, R. M.; Liu, S.; Banda, G.; Lentini, S. P.; Das, S.; Xu, Q.; Keats, J.; Wang, F.; Wardwell, S.; Ning, Y.; Snodgrass, J. T.; Broudy, M. I.; Russian, K.; Daley, G. Q.; Iuliucci, J.; Dalgarno, D. C.; Clackson, T.; Sawyer, T. K.; Shakespeare, W. C. *J. Med. Chem.* **2009**, *52*, 4743.
- Homsy, J.; Cubitt, C. L.; Zhang, S.; Munster, P. N.; Yu, H.; Sullivan, D. M.; Jove, R.; Messina, J. L.; Daud, A. I. *Melanoma Res.* **2009**, *19*, 167.
- Lafleur, K.; Huang, D.; Zhou, T.; Caffisch, A.; Nevado, C. *J. Med. Chem.* **2009**, *52*, 6433.
- Lee, K.; Kim, J.; Jeong, K. W.; Lee, K. W.; Lee, Y.; Song, J. Y.; Kim, M. S.; Lee, G. S.; Kim, Y. *Bioorg. Med. Chem.* **2009**, *17*, 3152.
- Boschelli, D. H.; Wang, D.; Wang, Y.; Wu, B.; Honores, E. E.; Barrios Sosa, A. C.; Chaudhary, I.; Golas, J.; Lucas, J.; Boschelli, F. *Bioorg. Med. Chem. Lett.* **2010**, *20*, 2924.
- Dalgarno, D.; Stehle, T.; Narula, S.; Schelling, P.; van Schravendijk, M. R.; Adams, S.; Andrade, L.; Keats, J.; Ram, M.; Jin, L.; Grossman, T.; MacNeil, I.; Metcalf, C., III; Shakespeare, W.; Wang, Y.; Keenan, T.; Sundaramoorthi, R.; Bohacek, R.; Weigele, M.; Sawyer, T. *Chem. Biol. Drug Des.* **2006**, *67*, 46.
- Wang, Y.; Metcalf, C. A., III; Shakespeare, W. C.; Sundaramoorthi, R.; Keenan, T. P.; Bohacek, R. S.; van Schravendijk, M. R.; Violette, S. M.; Narula, S. S.; Dalgarno, D. C.; Haraldson, C.; Keats, J.; Liou, S.; Mani, U.; Pradeepan, S.; Ram, M.; Adams, S.; Weigele, M.; Sawyer, T. K. *Bioorg. Med. Chem. Lett.* **2003**, *13*, 3067.
- Legraverend, M.; Grierson, D. S. *Bioorg. Med. Chem.* **2006**, *14*, 3987.
- Chang, Y. T.; Wignall, S. M.; Rosania, G. R.; Gray, N. S.; Hanson, S. R.; Su, A. I.; Merlie, J., Jr.; Moon, H. S.; Sangankar, S. B.; Perez, O.; Heald, R.; Schultz, P. G. *J. Med. Chem.* **2001**, *44*, 4497.
- Chiosis, G.; Timaul, M. N.; Lucas, B.; Munster, P. N.; Zheng, F. F.; Sepp-Lorenzino, L.; Rosen, N. *Chem. Biol.* **2001**, *8*, 289.
- Gundersen, L. L.; Nissen-Meyer, J.; Spilsberg, B. *J. Med. Chem.* **2002**, *45*, 1383.
- Penning, T. D.; Chandrakumar, N. S.; Desai, B. N.; Djuric, S. W.; Gasiecki, A. F.; Malecha, J. W.; Miyashiro, J. M.; Russell, M. A.; Askonas, L. J.; Gierse, J. K.; Harding, E. I.; Highkin, M. K.; Kachur, J. F.; Kim, S. H.; Villani-Price, D.; Pyla, E. Y.; Ghoreishi-Haack, N. S.; Smith, W. G. *Bioorg. Med. Chem. Lett.* **2003**, *13*, 1137.
- Chapman, E.; Ding, S.; Schultz, P. G.; Wong, C. H. *J. Am. Chem. Soc.* **2002**, *124*, 14524.
- Altmann, E.; Cowan-Jacob, S. W.; Missbach, M. *J. Med. Chem.* **2004**, *47*, 5833.
- Raboison, P.; Lugnier, C.; Muller, C.; Reimund, J. M.; Schultz, D.; Pinna, G.; Le Bec, A.; Basaran, H.; Desaubry, L.; Gaudiot, F.; Seloum, M.; Bourguignon, J. J. *Eur. J. Med. Chem.* **2003**, *38*, 199.
- Baraldi, P. G.; Fruttarolo, F.; Tabrizi, M. A.; Romagnoli, R.; Preti, D.; Bovero, A.; Pineda de Las Infantas, M. J.; Moorman, A.; Varani, K.; Borea, P. A. *J. Med. Chem.* **2004**, *47*, 5535.
- Cheng, D.; Ding, Q.; Han, D.; Gray, N. S.; Zhang, G.; Dai, C.; Dong, H.; Guo, B. Z.; Qiang, D.; Schiander, G. N.; Gray, M. S. Patent WO2005016528, 2005; *Chem. Abstr.* **2005**, *142*, 261551.
- Winzeler, E.; Gray, N. S.; Han, D.; Cheng, D. Patent WO2008094737, 2008; *Chem. Abstr.* **2008**, *149*, 246557.
- Chen, G.; Zheng, S.; Luo, X.; Shen, J.; Zhu, W.; Liu, H.; Gui, C.; Zhang, J.; Zheng, M.; Puah, C. M.; Chen, K.; Jiang, H. *J. Comb. Chem.* **2005**, *7*, 398.
- Carraro, F.; Naldini, A.; Pucci, A.; Locatelli, G. A.; Maga, G.; Schenone, S.; Bruno, O.; Ranise, A.; Bondavalli, F.; Brullo, C.; Fossa, P.; Menozzi, G.; Mosti, L.; Modugno, M.; Tintori, C.; Manetti, F.; Botta, M. *J. Med. Chem.* **2006**, *49*, 1549.
- Liu, Y.; Bishop, A.; Witucki, L.; Kraybill, B.; Shimizu, E.; Tsien, J.; Ubersax, J.; Blethrow, J.; Morgan, D. O.; Shokat, K. M. *Chem. Biol.* **1999**, *6*, 671.
- Alvarez, R. H.; Kantarjian, H. M.; Cortes, J. E. *Cancer* **2006**, *107*, 1918.
- Stevenson, J. M.; Mulready, P. D. *J. Am. Chem. Soc.* **2003**, *125*, 1437.
- <http://accelrys.com/events/webinars/discovery-studio-25/>.
- Morris, G. M.; Goodsell, D. S.; Halliday, R. S.; Huey, R.; Hart, W. E.; Belew, R. K.; Olson, A. J. *J. Comput. Chem.* **1998**, *19*, 1639.
- Huang, H.; Liu, H.; Chen, K.; Jiang, H. *J. Comb. Chem.* **2007**, *9*, 197.